Supporting Information

Highly Efficient Room-Temperature Phosphorescence from Halogen-Bonding Assisted Doped Organic Crystals

Lu Xiao,[†,‡] *Yishi Wu,*[†] *Jianwei Chen,*[†,‡] *Zhenyi Yu,*[†,‡] *Yanping Liu,*[†,‡] *Jiannian Yao,*[†,‡] *and Hongbing Fu*[*,†,§,∥]

[†]Beijing National Laboratory for Molecular Sciences (BNLMS), Institute of chemistry, Chinese Academy of Sciences, Beijing 100190, People's Republic of China.

[‡]University of Chinese Academy of Sciences, Beijing 100049, People's Republic of China.

[§] Beijing Key Laboratory for Optical Materials and Photonic Devices (BKLOMPD), Department of Chemistry, Capital Normal University, Beijing 100048, People's Republic of China

[∥] Tianjin Key Laboratory of Molecular Optoelectronic Sciences, Department of Chemistry, Tianjin University, and Collaborative Innovation Center of Chemical Science and Engineering (Tianjin), Tianjin 300072, People's Republic of China

Corresponding Author

*E-mail: hbfu@cnu.edu.cn; hongbing.fu@iccas.ac.cn.

Experimental Sections

Scheme S1. Synthesis of dbm-R Dyes.

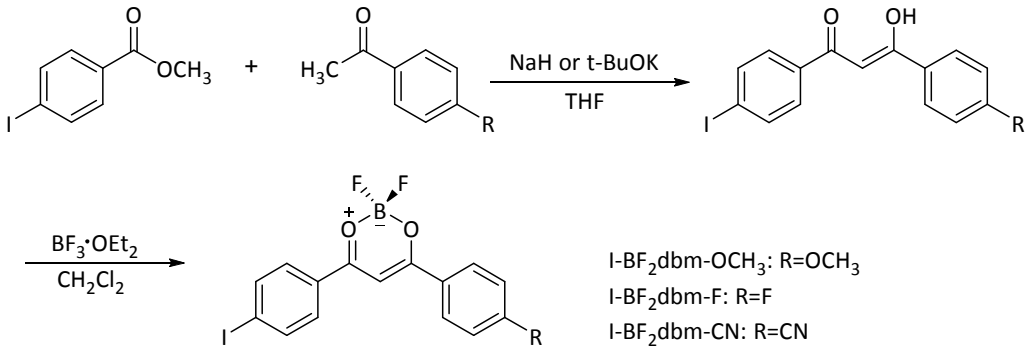

Synthesis of I-BF_2dbm-R Dyes.

Synthesis of **I-BF_2dbm-OCH_3**. 1-(4-methoxyphenyl)ethanone (750mg, 5 mmol) and methyl 4-iodobenzoate (1.31 g, 5 mmol) was added into a 250 mL round-bottom. The flask was purged with argon before adding 120 mL of THF as solvent. After stirring the mixture for 8 min, a suspension containing NaH (200 mg, 8.3 mmol) in THF (10 mL) was added dropwise at room temperature. The mixture was then heated to 80℃ and stirred in the dark overnight. After cooling to room temperature, the reaction was quenched by adding aqueous NH_4Cl (3 mL). The aqueous phase was extracted with CH_2Cl_2. The combined organic layers were washed with distilled water and brine several times. After drying, the solvent was then removed under reduced pressure. The residue was purified by silica gel chromatography using petroleum ether/dichloromethane (2:1 v/v) as the eluent to obtain a white solid. Then the crude product was dissolved in 100mL dichloromethane, and boron trifluoride diethyl etherate (630 μL, 5 mmol) was added under argon. The mixture was stirred at room temperature in the dark overnight. The solvent was removed under reduced pressure. The residue was recrystallized over hexanes/dichloromethane to give I-BF_2dbm-OCH_3 as a bright yellow powder (760 mg, 83%). ^{1}H NMR (400 MHz, CD_2Cl_2) δ 8.15 (d, J = 9.1 Hz, 2H), 7.93 (d, J = 8.7 Hz, 2H), 7.81 (d, J = 8.7 Hz, 2H), 7.16 – 6.99 (m, 3H), 3.93 (s, 3H); ^{13}C NMR (101 MHz, CD_2Cl_2) δ 182.81, 180.39, 166.27, 138.54, 131.76, 129.55, 123.98, 114.83, 102.81, 92.65, 55.91; HR-EI-MS m/z calculated for $C_{16}H_{12}BF_2IO_3$ $[M]^+$: 427.9892; m/z (found): 427.9896

Synthesis of **I-BF_2dbm-F**. 1-(4-fluorophenyl)ethanone (691mg, 5 mmol) and methyl 4-iodobenzoate (1.31 g, 5 mmol) was added into a 250 mL round-bottom. The flask was purged with argon before adding 120 mL of THF as a solvent. After stirring the mixture for 8 min, a suspension containing NaH (200 mg, 8.3 mmol) in THF (10 mL) was added dropwise at room temperature. The mixture was then stirred at RT in the dark for 24 h. The following procedure are the same as dbm-OCH_3. The boronation mixture was recrystallized from hexanes/ dichloromethane to give I-BF_2dbm-F as a yellow solid (390

mg, 71 %). ^{1}H NMR (400 MHz, CD_2Cl_2) δ 8.19 (dd, J = 9.0, 5.2 Hz, 2H), 7.96 (d, J = 8.7 Hz, 2H), 7.88 – 7.76 (m, 2H), 7.27 (t, J = 8.6 Hz, 2H), 7.13 (s, 1H); 13C NMR (101 MHz, CD_2Cl_2) δ 182.49, 168.63, 166.05, 138.73, 131.85, 131.40, 129.82, 128.23, 116.80, 116.58, 103.81, 93.33; HR-EI-MS m/z calculated for $C_{15}H_9BF_3IO_2$ $[M]^+$: 415.9692; m/z (found): 415.9698

Synthesis of **I-BF$_2$dbm-CN**. 4-acetylbenzonitrile (730mg, 5 mmol) was added into a 250 mL round-bottom. The flask was purged with argon before adding 7mL of t-BuOK (1M, THF) and 120 mL of THF as a solvent. After stirring the mixture at room temperature for 3 h, methyl 4-iodobenzoate (1.31 g, 5 mmol) was added. The mixture was then stirred at RT in the dark for 24 h. The following procedure are the same as dbm-OCH_3. The boronation mixture was recrystallized over hexanes/dichloromethane to give I-BF_2dbm-CN as a dark yellow solid (350 mg, 70%). ^{1}H NMR (400 MHz, CD_2Cl_2) δ 8.22 (d, J = 8.6 Hz, 2H), 7.99 (d, J = 8.7 Hz, 2H), 7.93 – 7.79 (m, 4H), 7.20 (s, 1H); ^{13}C NMR (101 MHz, CD_2Cl_2) δ 184.41, 181.38, 138.94, 135.67, 132.89, 131.02, 130.12, 129.07, 118.16, 117.44, 104.98, 94.49; HR-EI-MS m/z calculated for $C_{16}H_9BF_2INO_2$ $[M]^+$: 422.9739; m/z (found): 422.9745

Characterization.

^{1}H NMR (400 MHz) and ^{13}C NMR (101 MHz) spectra were recorded in deuterated solvents on a Bruker ADVANCE 400 NMR Spectrometer. High resolution mass spectra (HRMS) were determined on on a Bruker APEX II mass spectrometer. UV-vis spectra were obtained from a Shimidzu UV-3600. The photoluminescence (PL) spectra were measured on Horiba FluoroMax-4 spectrophotometer. The PL quantum yields were measured absolutely by using an integrating sphere[1] at an excitation wavelength of 380 nm. The fluorescence (phosphorescence) lifetimes were measured on an Edinburgh FLS980 spectrometer. The X-ray diffraction (XRD) patterns were measured by a D/max 2400 X-ray diffractometer with Cu Kα radiation (λ=1.54050 Å) operated in the 2θ range from 3° to 30°.

Nanosecond flash photolysis.

The THF output (355 nm) of the Nd:YAG laser (Continuum Surelite II, 7 ns fwhm) was used for direct excitation. A pulsed xenon arc lamp was used to provide the analyzing light. The configuration of the monitoring light with respect to the excitation laser pulse is a perpendicular geometry. The liquid samples (1.0 cm quartz cell) were settled on the platform at the intersection of the monitoring light and the excitation pulse. All the samples are optically dilute at the laser excitation wavelength. The signals were detected by the Edinburgh LP920 and recorded on the Tektronix TDS 3012B oscilloscope and computer. The triplet lifetimes were obtained by kinetic analysis of the transient absorption. The dissolved oxygen was removed through bubbling with high purity N_2 for ~30 min. All the spectra were measured at room temperature if no further notification.

Sample preparation for PMMA films and I-BF$_2$dbm-R/IBN doped crystals.

The PMMA thin films were fabricated on a quartz slide by spin coating from a $CHCl_3$ solution (50 mg/mL) of I-BF_2dbm-R dyes and PMMA (1wt% mixture of I-BF_2dbm-R to PMMA) onto a quartz plate at 1500 rpm for 60 seconds. The I-BF_2dbm-R/Iph-C≡N doped crystals were prepared by simple

drop casting from a $CHCl_3$ solution (10 mg/mL) of I-BF_2dbm-R dyes and Iph-C≡N (1wt% mixture of I-BF_2dbm-R to Iph-C≡N) onto a quartz plate.

Theoretical calculations.

All the calculations are performed using Gaussion09 software package.[2] The I-BF_2dbm-R molecules are computationally modeled using density functional theory (DFT) calculations at the B3LYP/DEF2-SVP level in the gas phase. The solid phase calculations are performed using an ONIOM model for the The I-BF_2dbm-R/Iph-C≡N doped crystals, with one central I-BF_2dbm-R molecule and eight nearest Iph-C≡N molecules as high layer calculated using the same method as the gas phase calculations and all the surrounding molecules as low layer calculated using MM method with the UFF force field. The I-BF_2dbm-R/Iph-C≡N doped crystal is built as a 363 Iph-C≡N supercell, with two Iph-C≡N molecules replaced by one central I-BF_2dbm-R molecule. The geometry optimization is carried out with all the Iph-C≡N molecules frozen.

Measurement of singlet oxygen yield and estimation the ISC efficiency.

Through continuous photolysis procedure, the quantum yield for generation of singlet oxygen has been described as below. (Diwu Z, et al. *J. Photochem. Photobiol. A: Chem.* **1992**, 64, 273.) Briefly, 9,10-diphenylanthracene (DPA) was used as a substrate to intercept singlet oxygen because of its nonradiative deactivation. The consumption of singlet oxygen in air-saturated CH_2Cl_2 solution was measured under 405 nm laser irradiation. The concentration of DPA was prepared at ~ 1.6×10^{-4} M. To ensure that an equal number of photons were absorbed at the same irradiation time in all experiments, the absorption of each photosensitizer was adjusted to 0.3 in a 1 cm cell at the wavelength of 405 nm. Therefore, the DPA can efficiently intercept the singlet oxygen. hypocrellin A (HA) (Φ_Δ= 0.84 in CH_2Cl_2) was used as the reference. The singlet oxygen quantum yield was calculated using the equation on:

$$\Phi_\Delta^S = \Phi_\Delta^R \times \frac{k^S/A^S}{k^R/A^R}$$

The *k* is the slope of singlet oxygen consumption, the A is the absorbance of photosensitizer at 405nm and the suffixes "S" and "R" refer to the sample and the reference, respectively. To eliminate the interfere of self-deactivation of DPA under 405 nm laser irradiation, the absorbance of DPA without photosensitizer was measured under the same condition. Then the ISC efficiency Φ_{ISC} of can be estimated using the equation:

$$\Phi_{ISC} = \Phi_\Delta/\eta$$

The η is the quantum efficiency of energy transfer from the triplet of I-BF_2dbm-R dyes to the triplet oxygen and is measured through the nanosecond transient absorption and estimated by $\eta = 1 - \tau_{air}/\tau_{N2}$. Then the ISC efficiency of the I-BF_2dbm-R dyes in CH_2Cl_2 solution was estimated to be $\Phi_{ISC,I\text{-}BF2dbm\text{-}OCH3}$= 0.44, $\Phi_{ISC,I\text{-}BF2dbm\text{-}F}$= 0.79 and $\Phi_{ISC,I\text{-}BF2dbm\text{-}CN}$= 0.83.

Supporting figures:

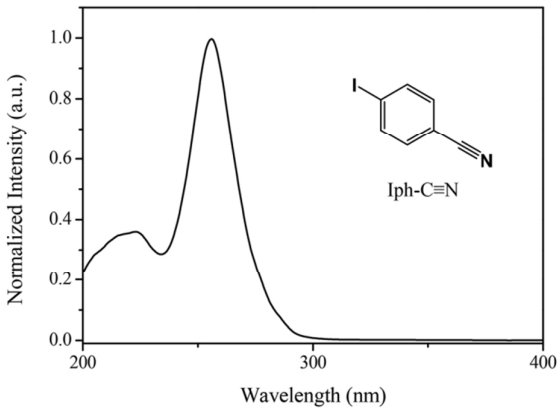

Figure S1. Normalized UV/vis absorption spectrum of Iph-C≡N in dilute CH_2Cl_2 solution.

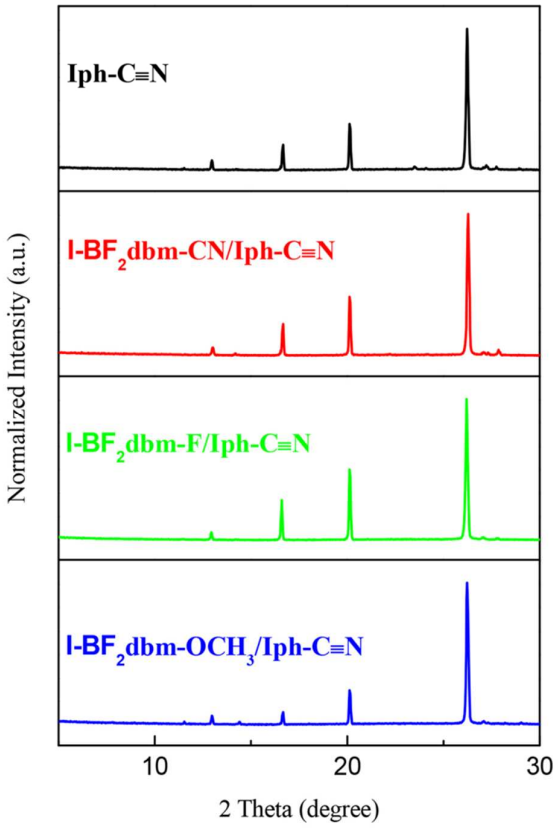

Figure S2. XRD results of I-BF_2dbm-R/Iph-C≡N doped crystals (1wt% mixture of I-BF_2dbm-R to Iph-C≡N) on a glass substrate.

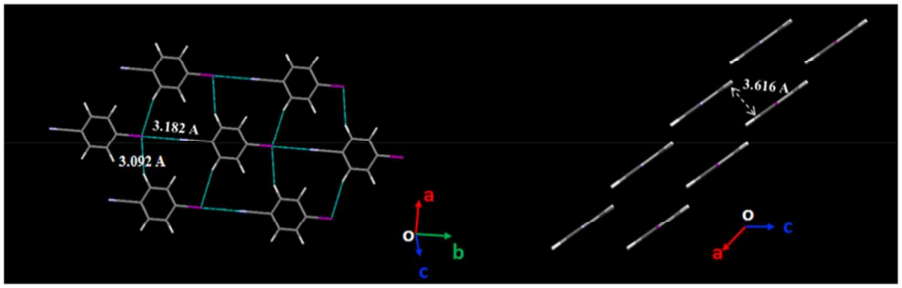

Figure S3. Intermolecular interactions and molecular packing styles in Iph-C≡N crystals.

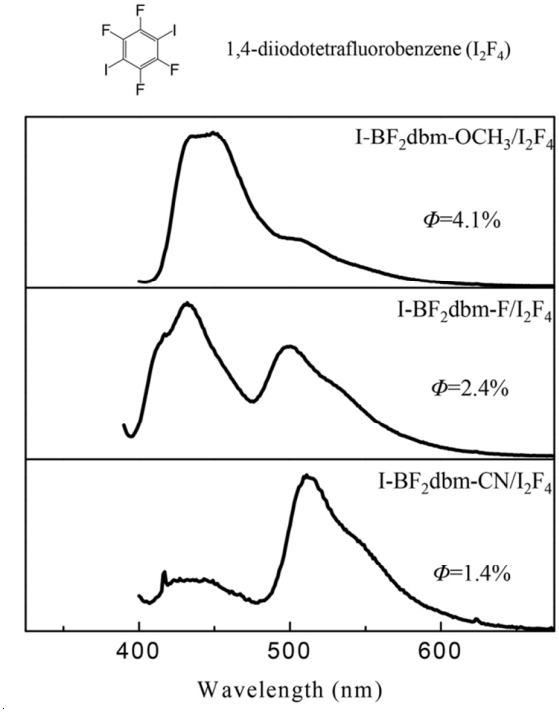

Figure S4. Emission spectra of I-BF_2dbm-R dyes doped in I_2F_4 crystals (1wt% mixture of I-BF_2dbm-R to I_2F_4).

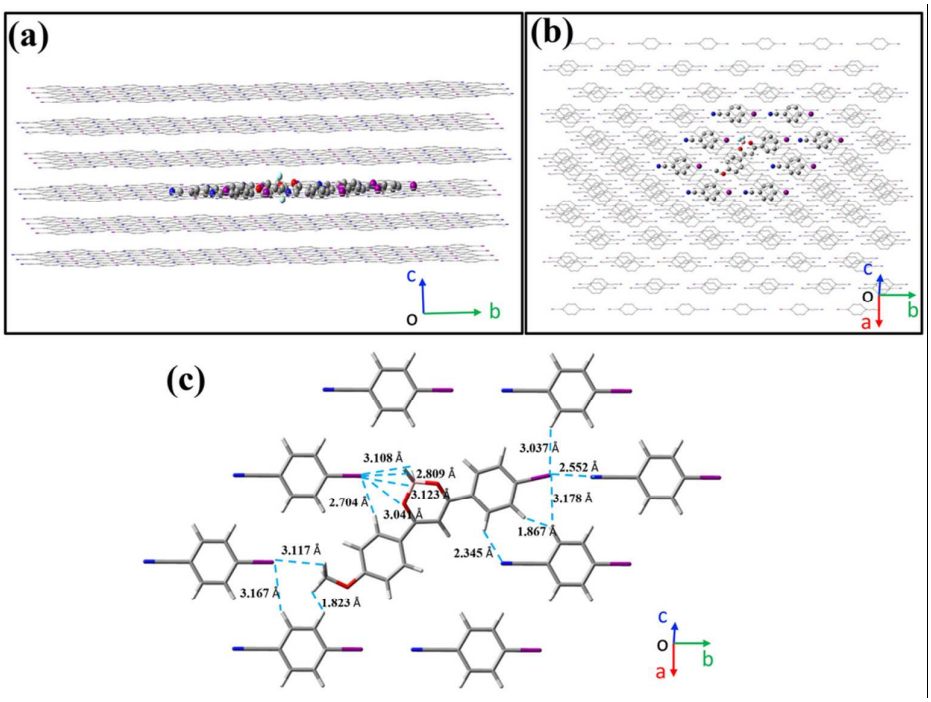

Figure S5. (a) and (b) optimized geometry model of the I-BF_2dbm-OCH_3 doped in Iph-C≡N. (c) The intermolecular interactions between I-BF_2dbm-OCH_3 and Iph-C≡N in I-BF_2dbm-OCH_3/Iph-C≡N doped crystal.

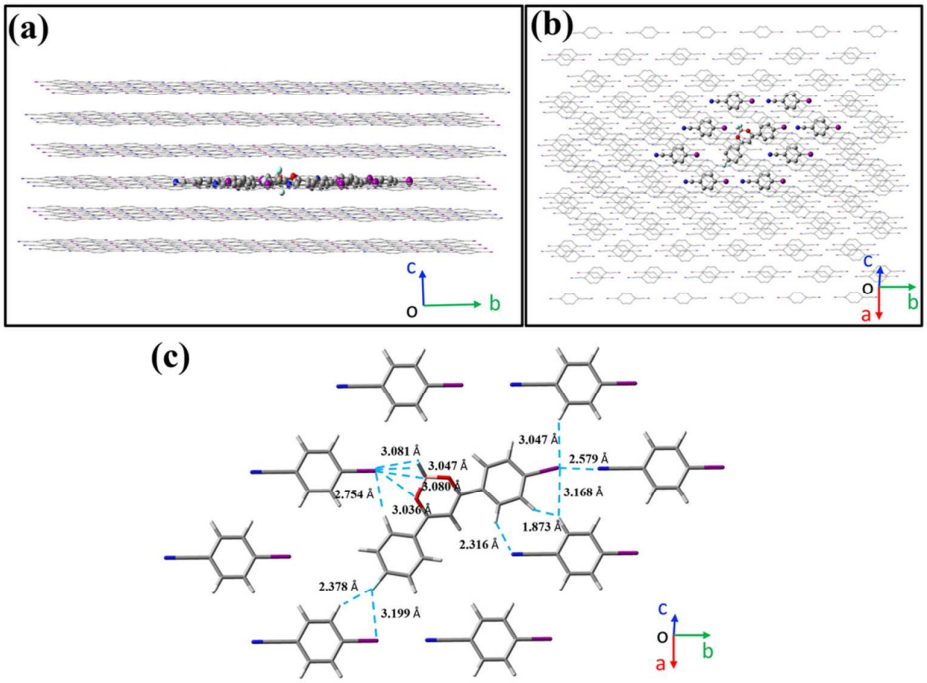

Figure S6. (a) and (b) optimized geometry model of the I-BF_2dbm-F doped in Iph-C≡N. (c) The intermolecular interactions between I-BF_2dbm-F and Iph-C≡N in I-BF_2dbm-F/Iph-C≡N doped crystal.

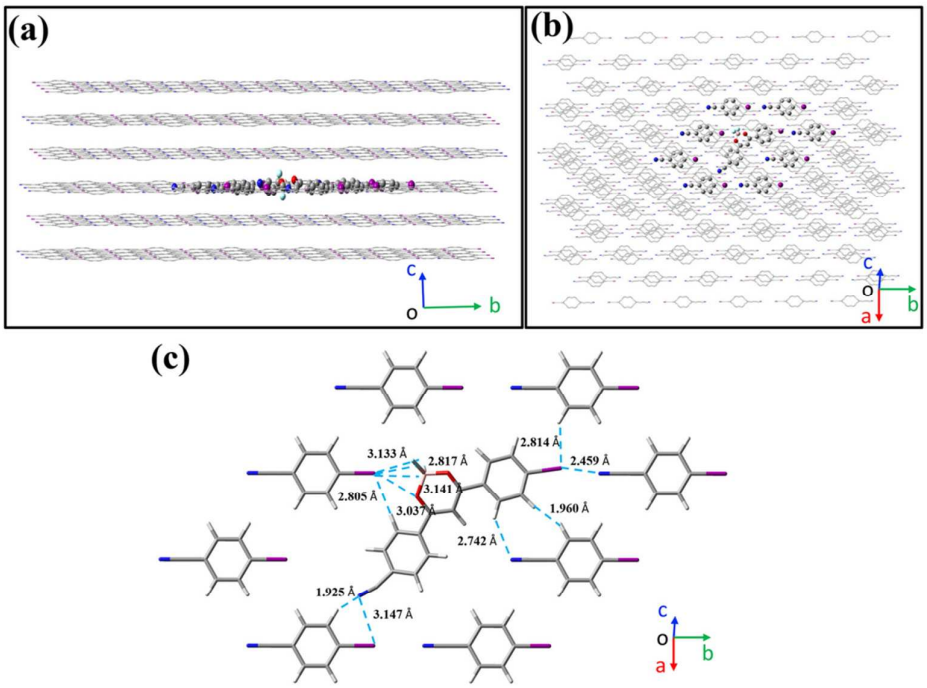

Figure S7. (a) and (b) optimized geometry model of the I-BF_2dbm-CN doped in Iph-C≡N. (c) The intermolecular interactions between I-BF_2dbm-CN and Iph-C≡N in I-BF_2dbm-CN/Iph-C≡N doped crystal.

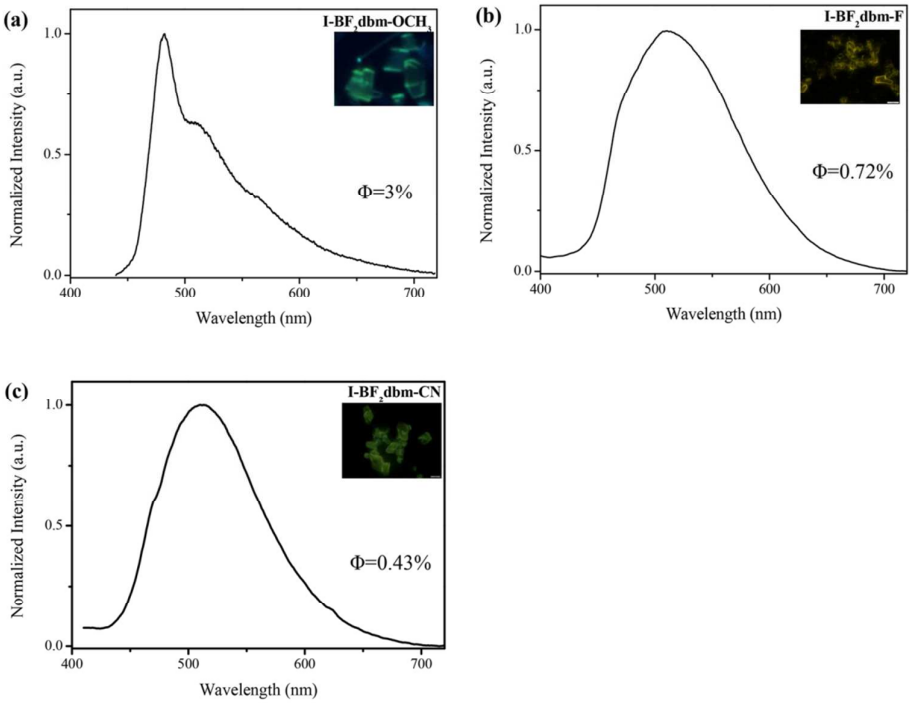

Figure S8. Normalized emission spectra of I-BF_2dbm-R dyes in crystals. Insets show the corresponding luminescence photographs photoluminescence quantum yields.

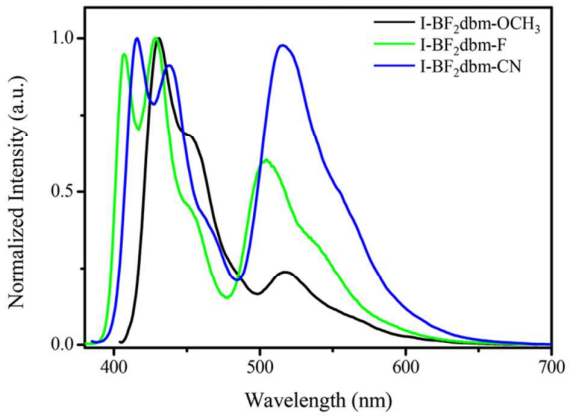

Figure S9. Normalized emission spectra of I-BF_2dbm-R dyes in PMMA films (1wt% mixture of I-BF_2dbm-R to PMMA) at 77K.

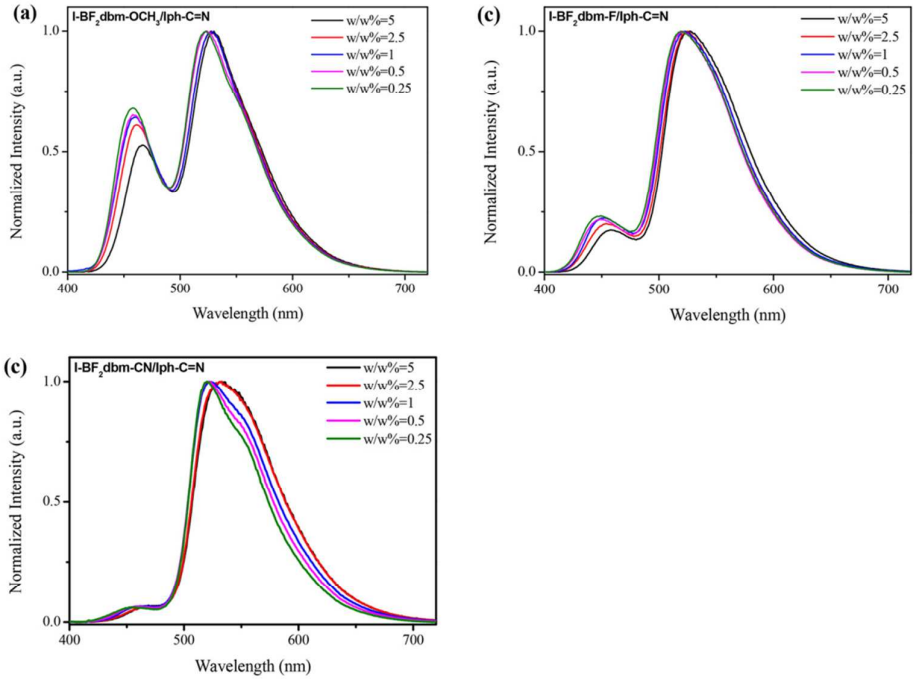

Figure S10. Normalized emission spectra of I-BF_2dbm-R/Iph-C≡N doped crystals at different mass ratios.

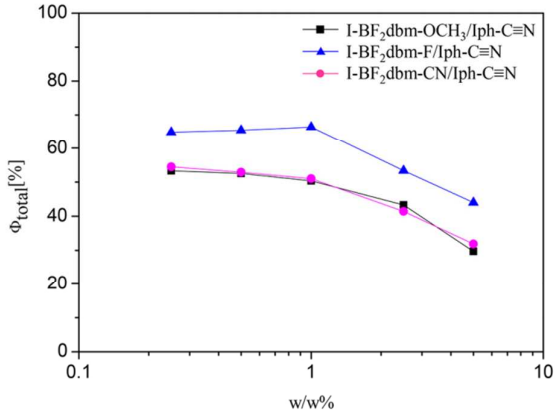

Figure S11. Total photoluminescence quantum yield of I-BF_2dbm-R/Iph-C≡N doped crystals at different mass ratios.

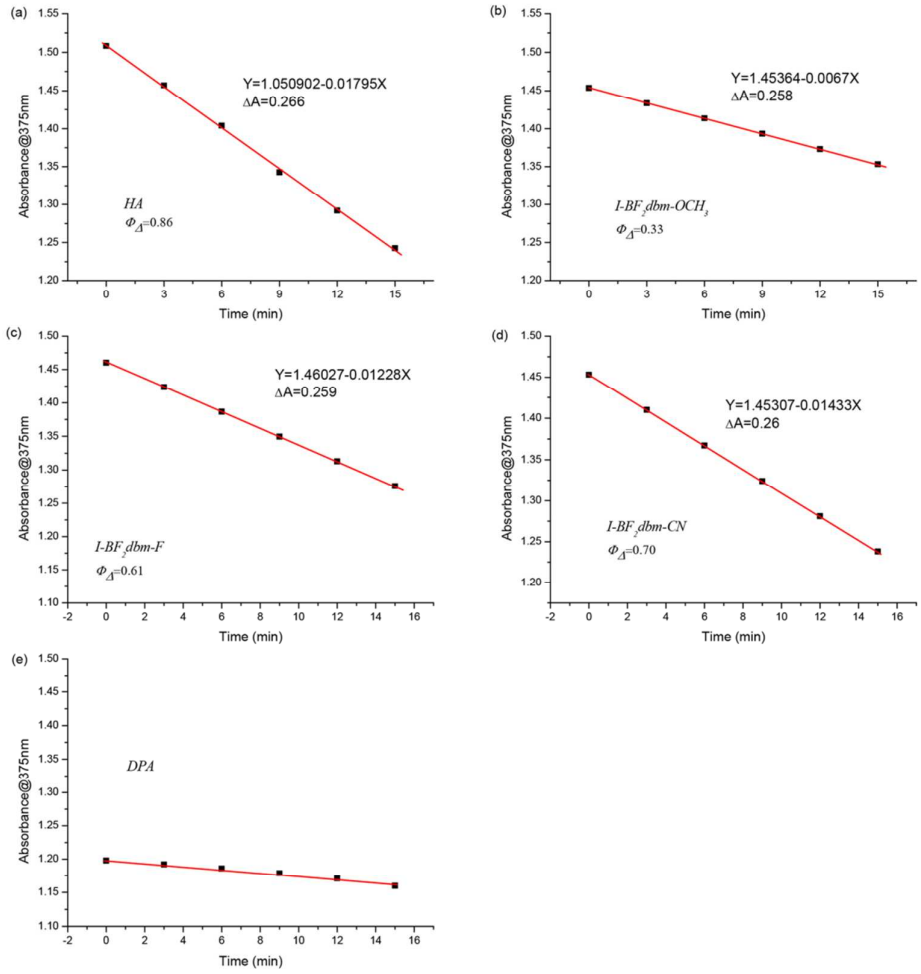

Figure S12. The decrease of the absorbance of DPA at 375 nm as a function of the irradiation time for (a) DPA with HA, (b) DPA with I-BF_2dbm-OCH_3, (c) DPA with I-BF_2dbm-F, (d) DPA with I-BF_2dbm-CN and (e) DPA without photosensitizer as a contrast. The linear fitting results are also shown.

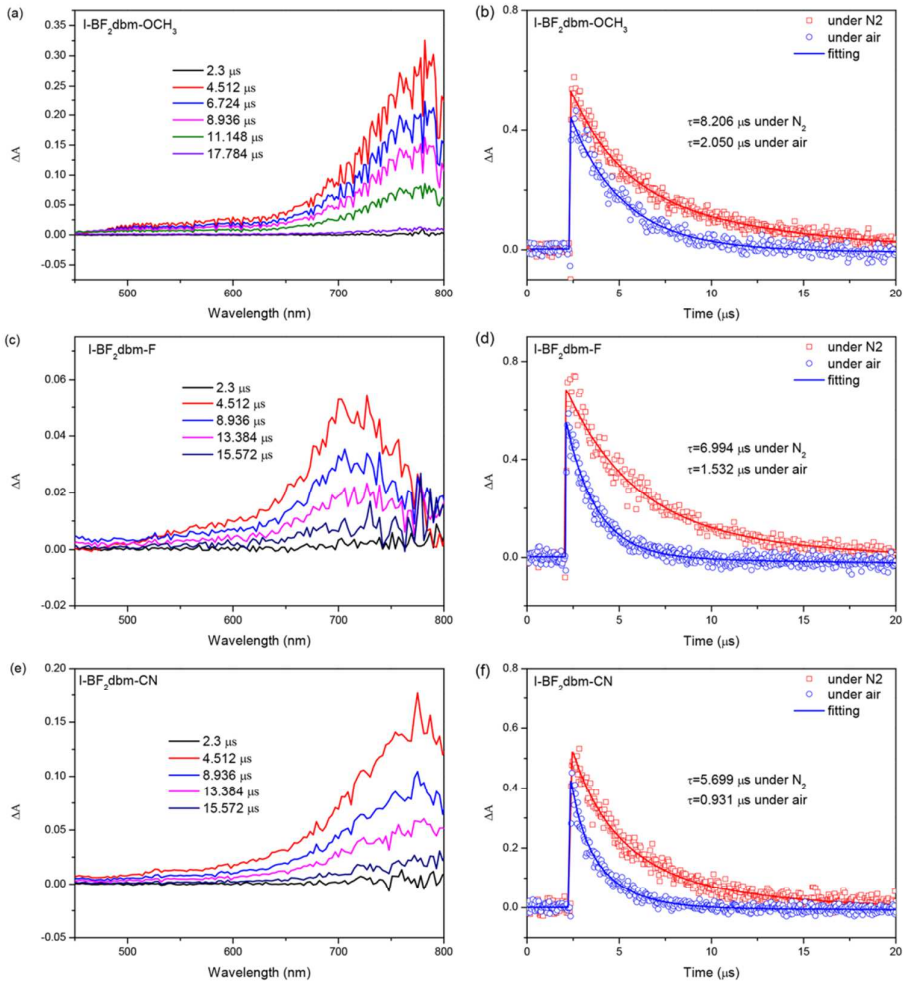

Figure S13. (a) The nanosecond transient absorption spectra and (b) time-absorption profiles at 750 nm under N_2 and under air recorded using flash photolysis of I-BF_2dbm-OCH_3 CH_2Cl_2 solution. (c) The nanosecond transient absorption spectra and (d) time-absorption profiles at 700 nm under N_2 and under air recorded using flash photolysis of I-BF_2dbm-F CH_2Cl_2 solution. (e) The nanosecond transient absorption spectra and (f) time-absorption profiles at 750 nm under N_2 and under air recorded using flash photolysis of I-BF_2dbm-CN CH_2Cl_2 solution. The measurements were upon excitation with 355 nm, ~2 mJ, and 0.45 cm diameter laser pulse.

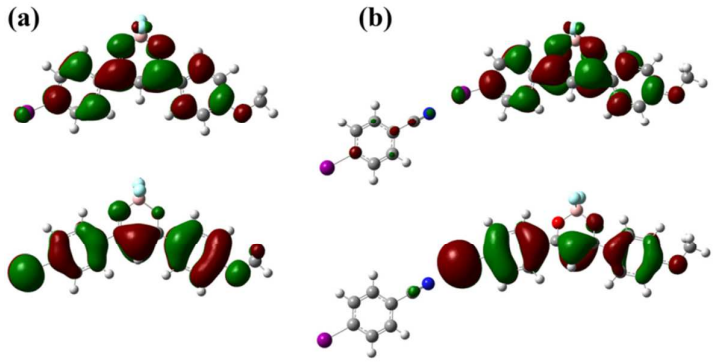

Figure S14. The highest occupied (down) and lowest unoccupied (up) natural transition orbitals (NTOs) diagrams of (a) isolated I-BF_2dbm-OCH_3 and (b) Iph-CN···I-BF_2dbm-OCH_3.

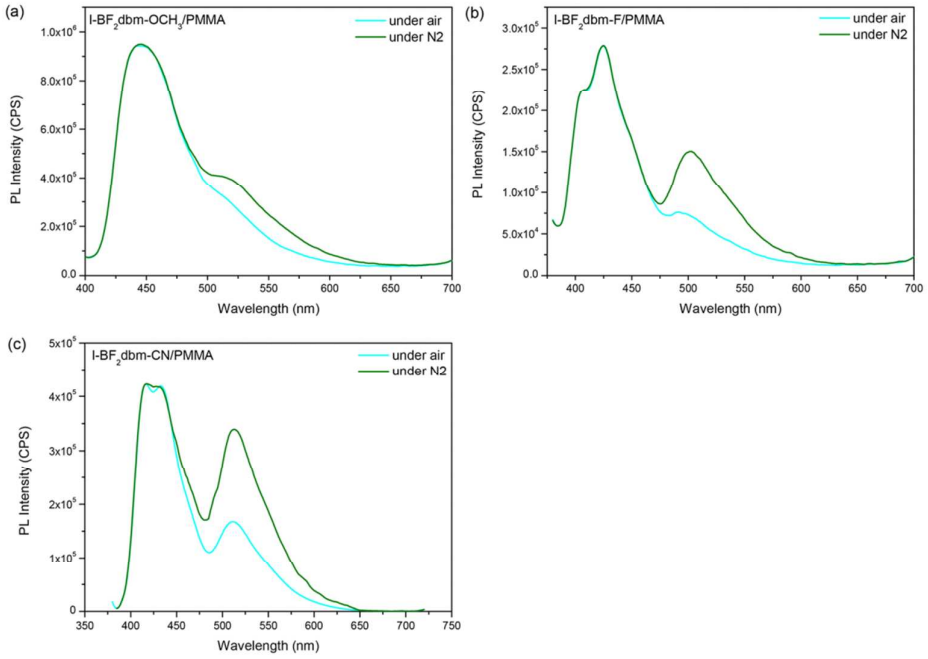

Figure S15. PL spectra of I-BF_2dbm-R dyes in PMMA film (1wt% mixture of I-BF_2dbm-R to PMMA) under air and N_2.

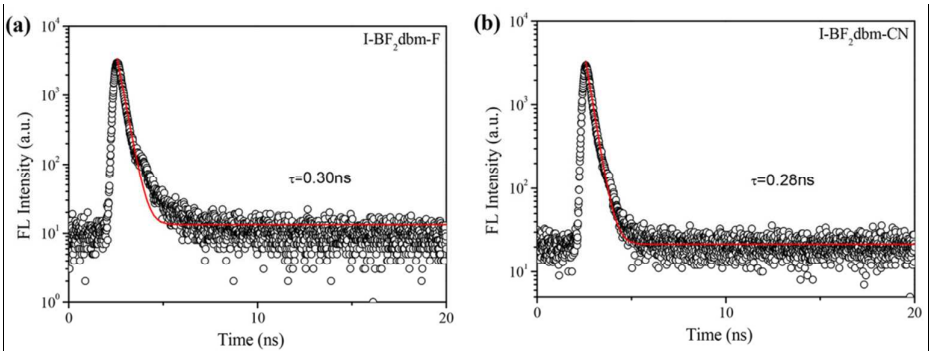

Figure S16. Fluorescence lifetime measurements for I-BF_2dbm-F and I-BF_2dbm-CN in CH_2Cl_2 solution.

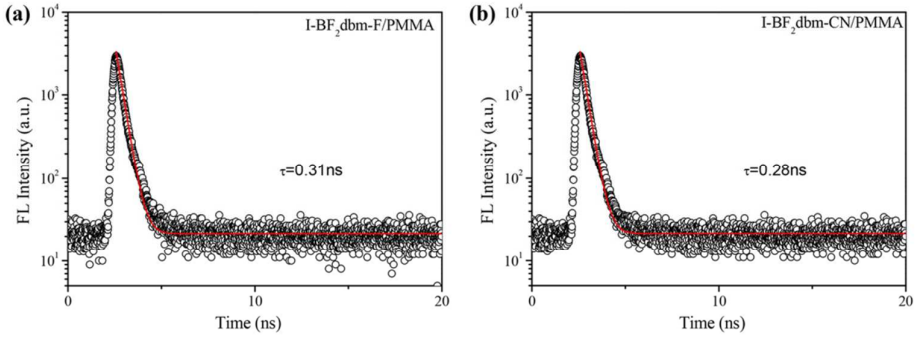

Figure S17. Fluorescence lifetime measurements for I-BF_2dbm-F and I-BF_2dbm-CN in PMMA film (1wt% mixture of I-BF_2dbm-R to PMMA).

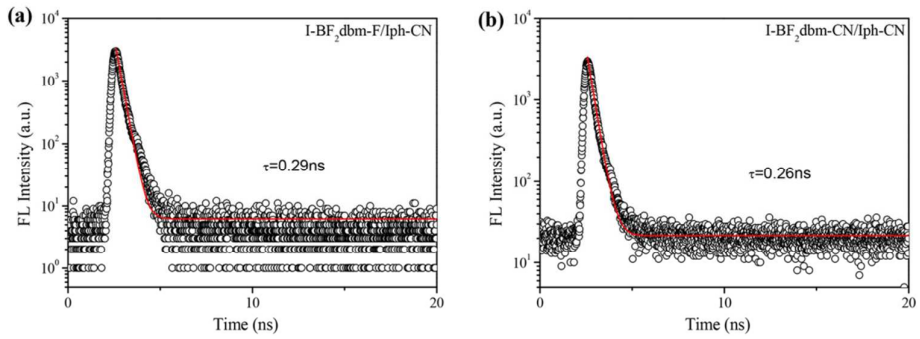

Figure S18. Fluorescence lifetime measurements for I-BF_2dbm-F and I-BF_2dbm-CN doped in Iph-C≡N crystals (1wt% mixture of I-BF_2dbm-R to Iph-C≡N).

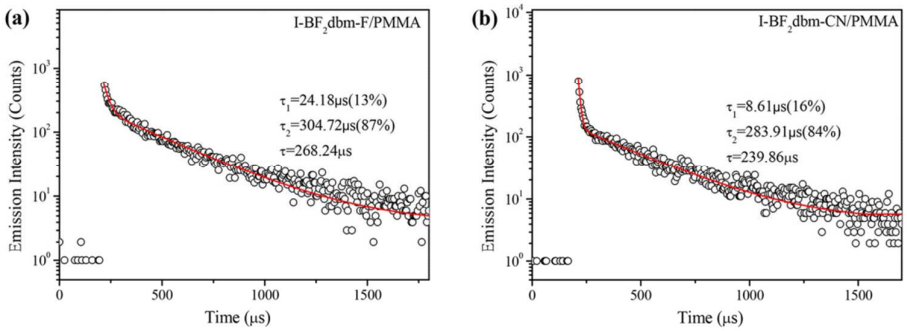

Figure S19. Phosphorescence lifetime measurements for I-BF_2dbm-F and I-BF_2dbm-CN in PMMA film (1wt% mixture of I-BF_2dbm-R to PMMA).

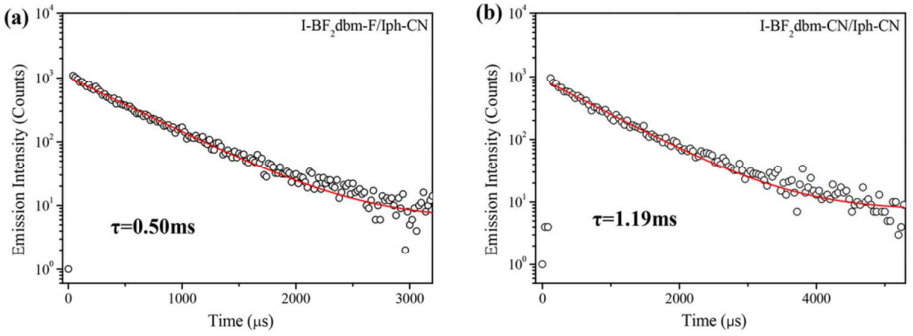

Figure S20. Phosphorescence lifetime measurements for I-BF_2dbm-F and I-BF_2dbm-CN doped in Iph-C≡N crystals (1wt% mixture of I-BF_2dbm-R to Iph-C≡N).

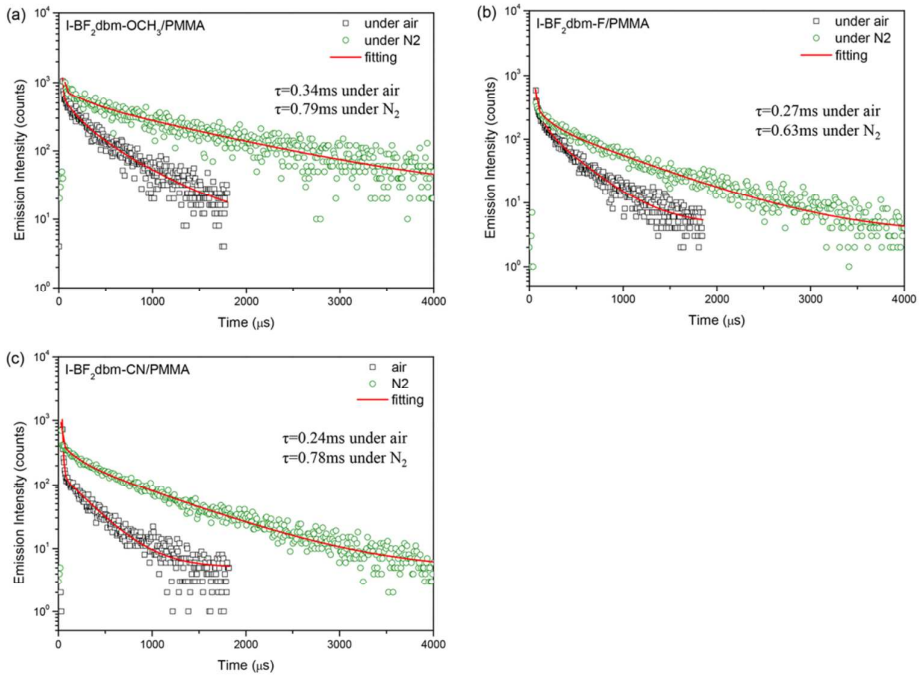

Figure S21. Phosphorescence lifetime measurements I-BF_2dbm-R dyes in PMMA film (1wt% mixture of I-BF_2dbm-R to PMMA) under air and N_2.

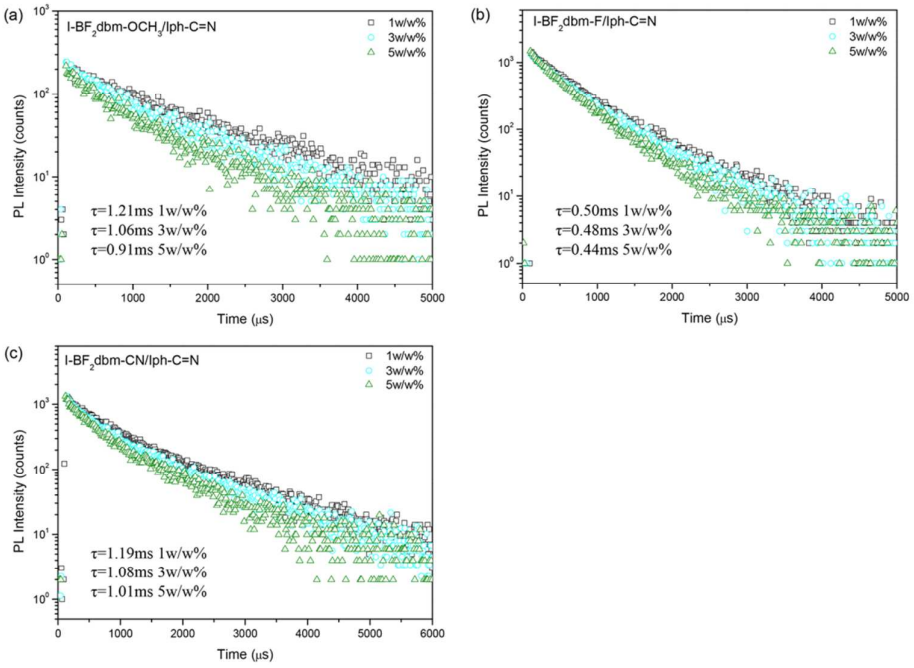

Figure S22. Phosphorescence lifetime measurements for I-BF_2dbm-R/Iph-C≡N doped crystals at different mass ratios.

NMR-Spectra

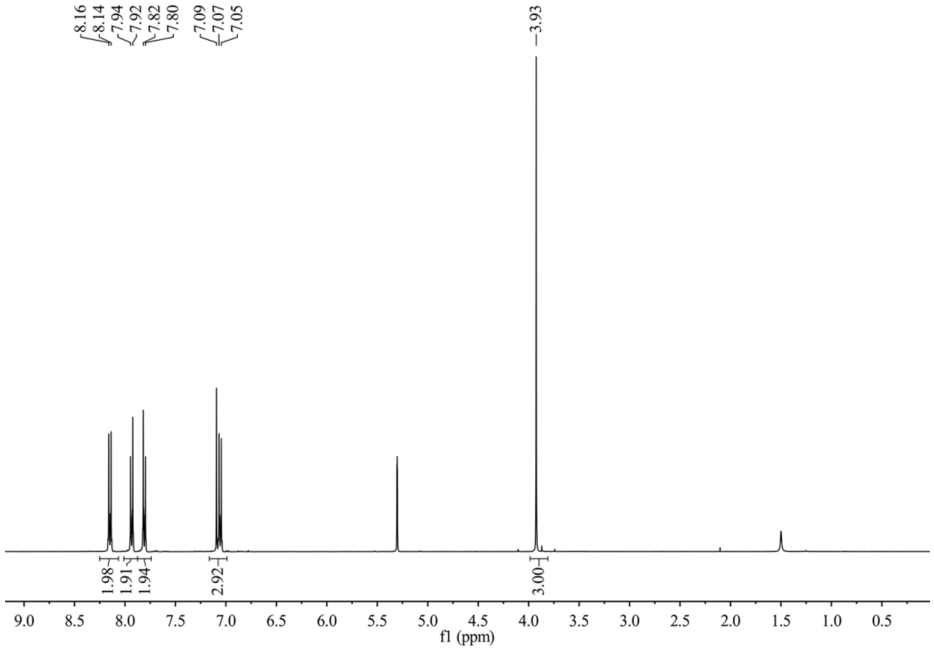

^{1}H NMR spectrum of **I-BF$_2$dbm-OCH$_3$** in CD_2CCl_2.

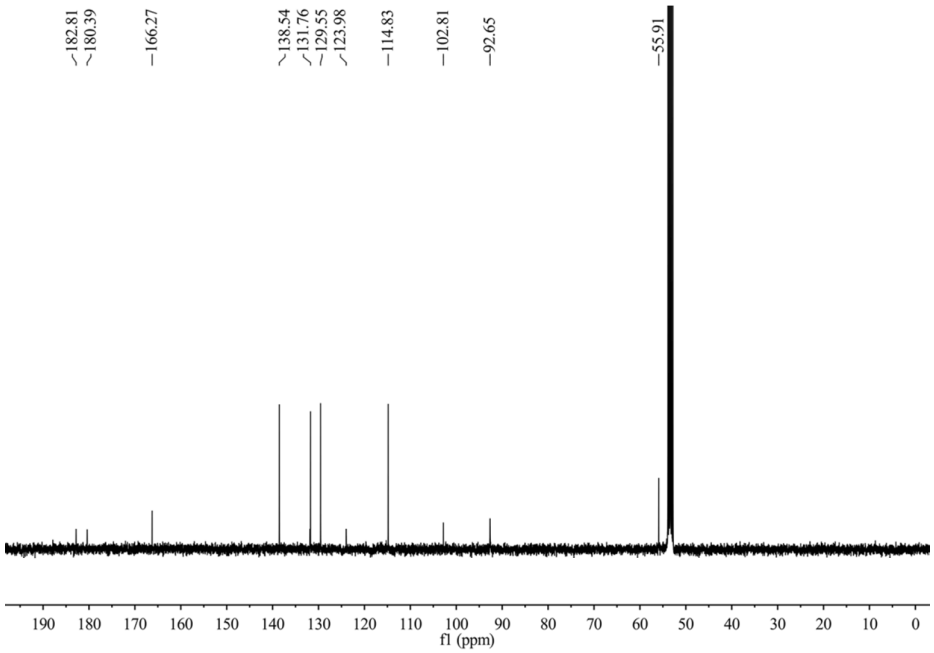

^{13}C NMR spectrum of **I-BF$_2$dbm-OCH$_3$** in CD_2CCl_2.

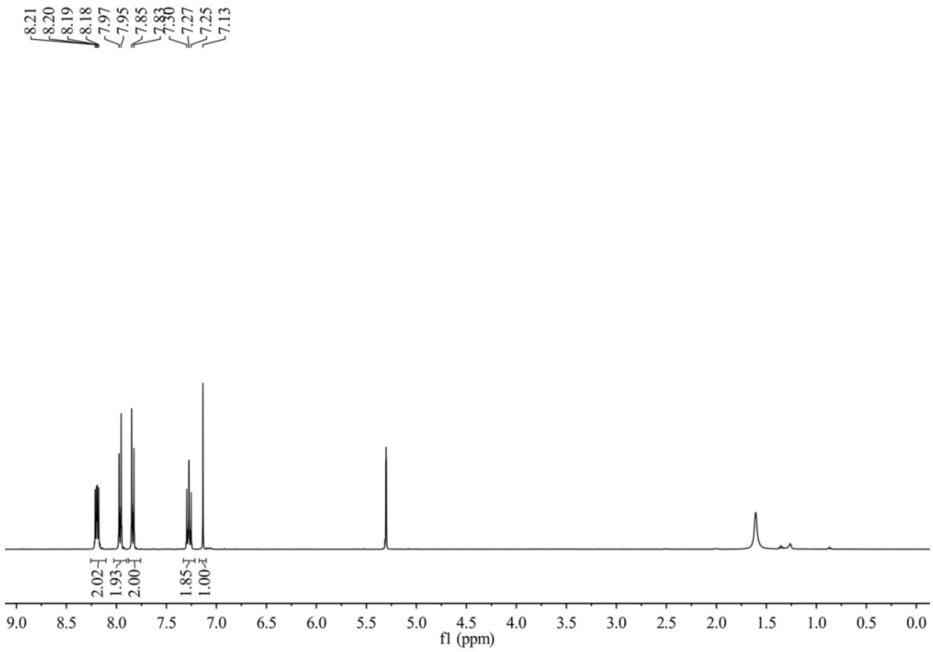

^{1}H NMR spectrum of **I-BF$_2$dbm-F** in CD_2CCl_2.

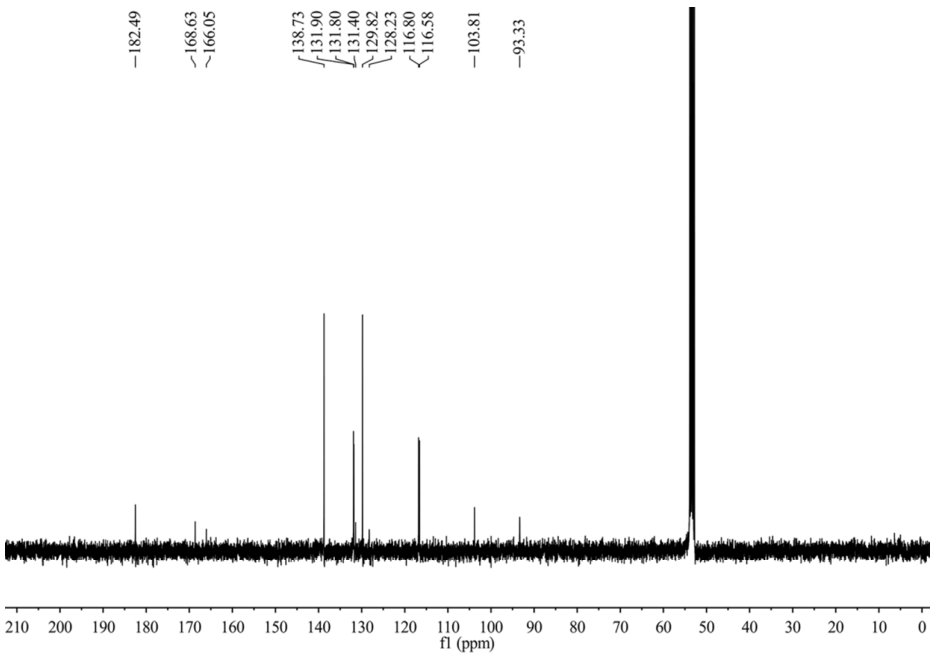

^{13}C NMR spectrum of **I-BF$_2$dbm-F** in CD_2CCl_2.

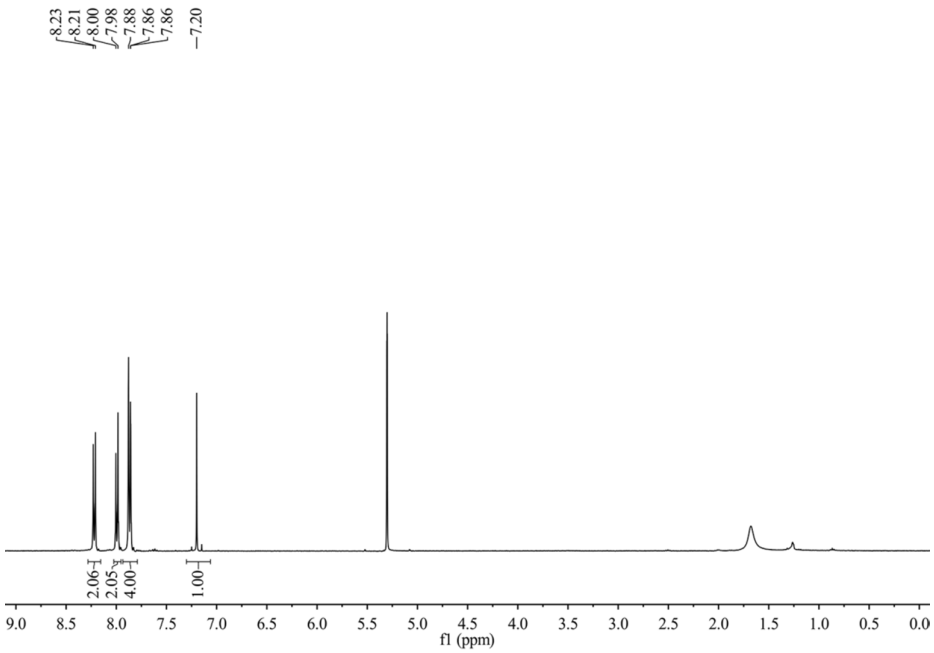

^{1}H NMR spectrum of **I-BF$_2$dbm-CN** in CD_2CCl_2.

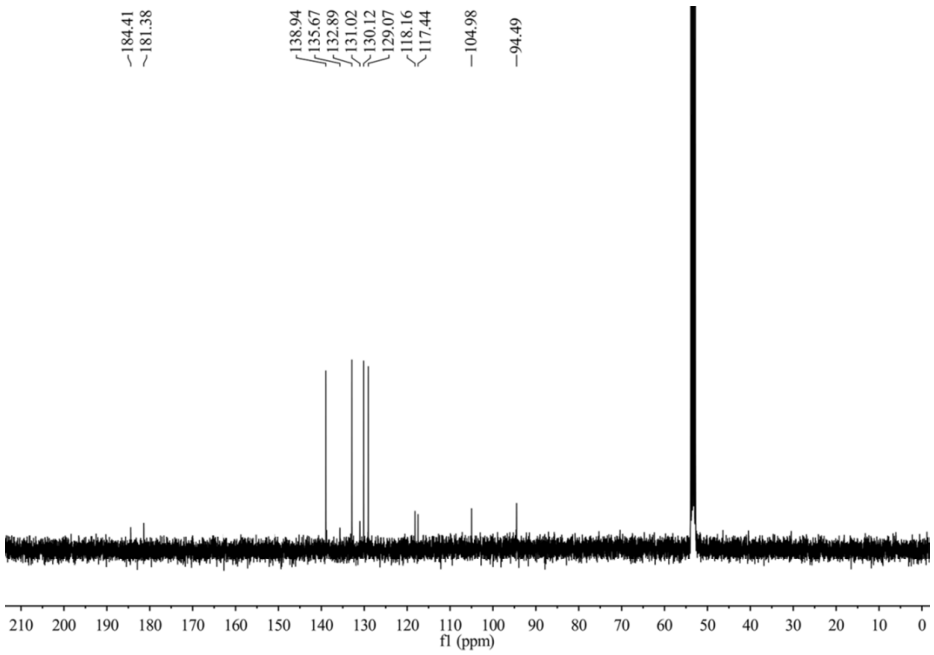

^{13}C NMR spectrum of **I-BF$_2$dbm-CN** in CD_2CCl_2.

References

1. Morris, W. A.; Sabat, M.; Butler, T.; DeRosa, C. A.; Fraser, C. L. Modulating Mechanochromic Luminescence Quenching of Alkylated Iodo Difluoroboron Dibenzoylmethane Materials. *J. Phys. Chem. C* **2016**, *120*, 14289-14300.

2. G. W. T. M. J. Frisch, H. B. Schlegel, G. E. Scuseria, M. A. Robb, J. R. Cheeseman, G. Scalmani, V. Barone, B. Mennucci, G. A. Petersson, H. Nakatsuji, M. Caricato, X. Li, H. P. Hratchian, A. F. Izmaylov, J. Bloino, G. Zheng, J. L. Sonnenberg, M. Hada, M. Ehara, K. Toyota, R. Fukuda, J. Hasegawa, M. Ishida, T. Nakajima, Y. Honda, O. Kitao, H. Nakai, T. Vreven, J. A. Montgomery, Jr., J. E. Peralta, F. Ogliaro, M. Bearpark, J. J. Heyd, E. Brothers, K. N. Kudin, V. N. Staroverov, R. Kobayashi, J. Normand, K. Raghavachari, A. Rendell, J. C. Burant, S. S. Iyengar, J. Tomasi, M. Cossi, N. Rega, J. M. Millam, M. Klene, J. E. Knox, J. B. Cross, V. Bakken, C. Adamo, J. Jaramillo, R. Gomperts, R. E. Stratmann, O. Yazyev, A. J. Austin, R. Cammi, C. Pomelli, J. W. Ochterski, R. L. Martin, K. Morokuma, V. G. Zakrzewski, G. A. Voth, P. Salvador, J. J. Dannenberg, S. Dapprich, A. D. Daniels, O. Farkas, J. B. Foresman, J. V. Ortiz, J. Cioslowski and D. J. Fox, Gaussian 09, Revision A.02, Gaussian, Inc., Wallingford CT, 2009.

The full names are listed for the references in the main text as follows.

Ref. 9: Kwon, M. S.; Yu, Y.; Coburn, C.; Phillips, A. W.; Chung, K.; Shanker, A.; Jung, J.; Kim, G.; Pipe, K.; Forrest, S. R.; Youk, J. H.; Gierschner, J.; Kim, J. Suppressing Molecular Motions for Enhanced Room-Temperature Phosphorescence of Metal-Free Organic Materials. *Nat. Commun.* **2015,** *6*, 8947.

Ref. 15: Yuan, W. Z.; Shen, X. Y.; Zhao, H.; Lam, J. W. Y.; Tang, L.; Lu, P.; Wang, C.; Liu, Y.; Wang, Z.; Zheng, Q.; Sun, J. Z.; Ma, Y.; Tang, B. Z. Crystallization-Induced Phosphorescence of Pure Organic Luminogens at Room Temperature. *J. Phys. Chem. C* **2010,** *114*, 6090-6099.

Ref. 26: Chen, X.; Xu, C.; Wang, T.; Zhou, C.; Du, J.; Wang, Z.; Xu, H.; Xie, T.; Bi, G.; Jiang, J.; Zhang, X.; Demas, J. N.; Trindle, C. O.; Luo, Y.; Zhang, G. Versatile Room-Temperature-Phosphorescent Materials Prepared from N-Substituted Naphthalimides: Emission Enhancement and Chemical Conjugation. *Angew. Chem. Int. Ed.* **2016,** *55*, 9872-9876.